A 2D NUMERICAL SIMULATION FOR NUCLEATION IN FLOW BOILING IN MICROCHANNEL HEAT SINK

Ahmed Jassim Shkarah [1, 2], Mohd Yusoff Bin Sulaiman [1], Md Razali bin Hj Ayob [1]
[1]Faculty of Mechanical Engineering, Universiti Teknikal Malaysia Melaka (UTeM), Melaka,
[2]Department of Mechanical Engineering, Thi-Qar University, 64001 Nassiriya, Iraq
Email : ahmedshkarah@gmail.com

*1.**ABSTRACT:** A numerical analytical system is suggested to entice bubble nucleation for the concept of flow boiling heat transfer in microchannels heat sink. In the microchannel using empirical theoretical correlations, flow boiling properties, bubble departure frequency, bubble growing time, waiting time and bubble departure diameter are devised and volume of fluid procedure is utilized to incite two phase flow and to track bubbles motion as well.*

2.INTRODUCTION

Many engineering complicated processes are included in flow boiling in a limited space[1]. Producing the two phase flow instability in flow boiling systems. The related mechanism about boiling is not fully understood yet. Uneven thermal stress on the heated surface and critical heat flux are the major effects of flow instability in microchannel. Description of flow instability process or measures of suppression the flow instability is the main topics to be studied. Two phase flow through microchannels has capability to give very high heat transfer rates in miniature heat exchangersAs boiling happens in microchannel bubbles nucleate at wall and fill the whole channel by growing large[2]. Nowadays the main focus is on the numerically simulate the boiling two phase flow in microchannel and analysis of different properties. To predict and understand the basic characteristic of flow boiling heat transfer, bubble dynamics is the most successful way to study. Bubble growth is mainly controlled by the momentum exchange between liquid and bubble after nucleate boiling being started on heated surface, then the bubble growth is due to evaporation through liquid vapor interface. The latency of vaporization is given by the heat diffusion from liquid. Ebullition or Boiling procedures mostly are governed by heat and mass diffusion. Ebullition process of bubble nucleation, growth and departure from heated surface is given in Fig.1.

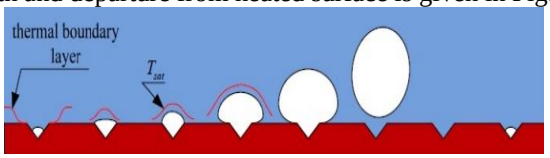

Fig.1 mechanism of nucleation and bubble growth and departure at an active cavity site.

3.NUMERICAL SIMULATION METHOD

A finite volume method has been followed to discretize the controlling equations for simulating bubble dynamics and heat transfer of forced connective flow boiling in a microchannel. Mass diffusion because of phase change is pointed out and Volume of fluid and heat is brought into use to arrest the moving interface b/w the liquid and vapor phases.The VOF process uses the Navier Stokes equations to replicate the two-phase flow boiling. The gravitational effects are neglected because of presence of dominant surface effects. Continuity and momentum equations become:

$$\frac{\partial \rho}{\partial t}+\nabla\bullet\left(\rho\vec{V}\right)=0 \qquad (2)$$

$$\frac{\partial\left(\rho\vec{V}\right)}{\partial t}+\nabla\bullet\left(\rho\vec{V}\vec{V}\right)=-\nabla p+\nabla\bullet\left[\mu\left(\nabla\vec{V}\right)\right]+S_M \quad (3)$$

The energy equation is :

$$\rho c_p\left(\frac{\partial T}{\partial t}+\vec{V}\bullet\nabla T\right)=\nabla\bullet k\nabla T+S_E \quad (4)$$

The finite volume method is suitable and evincing strength by using the conservation laws and treating the discontinuity at the interface. The finite volume method utilizes the volume integration for the conservation equations of mass and momentum and energy Eqs. (2-4) [13]:

$$\int_{cs}\left(\rho\vec{V}\right)\bullet\hat{n}\,dS=0 \quad (5)$$

$$\frac{\partial}{\partial t}\int_{cv}\rho\vec{V}d\forall+\int_{cs}\left(\rho\vec{V}\vec{V}\right)\bullet\hat{n}dS=-\int_{cs}p\hat{n}dS+\int_{cs}\left(\mu\nabla\vec{V}\right)\bullet\hat{n}dS+\int_{cv}S_M d\forall \quad (6)$$

$$\int_{cv}\frac{\partial}{\partial t}\left(\rho c_p T\right)d\forall+\int_{cs}\left(\rho c_p T\right)\left(\vec{V}\bullet\hat{n}\right)dS=\int_{cs}k\left(\nabla T\bullet\hat{n}\right)dS+\int_{cv}S_E d\forall \quad (7)$$

Using the finite volume method, the governing integral equations are discretized into the discretized cell to solve the computational domain numerically as shown in Figure 2:

$$\sum_{face}\rho\vec{V}\bullet\vec{A}=0 \qquad (8)$$

$$\frac{\partial}{\partial t}\sum_{face}\rho\vec{V}\Delta\forall+\sum_{face}\rho\vec{V}\vec{V}\bullet\vec{A}=-\sum_{face}p\bullet\vec{A}+\sum_{face}\mu\nabla\vec{V}\bullet\vec{A}+S_M\Delta\forall \quad (9)$$

$$\frac{\partial}{\partial t}\sum_{face}\rho c_p T\Delta\forall+\sum_{face}\rho c_p T\vec{V}\bullet\vec{A}=\sum_{face}k\nabla T\bullet\vec{A}+S_E\Delta\forall \quad (10)$$

Discretized equations fulfill the conservation properties for each cell.

$$\left(\rho\vec{V}\right)^{n+1}=\left(\rho\vec{V}\right)^{n}+\frac{\Delta t}{\Delta\forall}\left[-\sum_{face}\rho\vec{V}\vec{V}\bullet\vec{A}-\sum_{face}p\bullet\vec{A}+\sum_{face}\mu\nabla\vec{V}\bullet\vec{A}+S_M\Delta\forall\right]^{n+1} \quad (11)$$

$$\left(\rho c_p T\right)^{n+1}=\left(\rho c_p T\right)^{n}+\frac{\Delta t}{\Delta\forall}\left[-\sum_{face}\rho c_p T\vec{V}\bullet\vec{A}+\sum_{face}k\nabla T\bullet\vec{A}+S_E\Delta\forall\right]^{n+1} \quad (12)$$

Due to numerical diffusion mistakes of low order upwind schemes, terms used in Eq(10) are converted by QUICK scheme with third order. Central differencing formula having second-order accurate is used to discretize diffusion terms. The fully salient scheme with first order is implemented to the time integration since tiny time steps are utilized to assure calculated accuracy during the duplication. The ratio of liquid to vapor is greater in two phase flow boiling. Discontinuity of pressure gradients for boiling flows with promptly fluctuating densities at the liquid vapor interface is dealt by pressure interpolation scheme that uses PRESTO. PISO is

utilized by pressure velocity coupling calculations based on SIMPLE procedure (Semi-Implicit Method for Pressure-Linked Equations) method [13, 14]. One predictor and two corrector steps are included in PISO to enhance the efficiency of calculations, for the limitations of SIMPLE and SIMPLEC procedure is that when the pressure correction equations are answered, the new velocities and related fluxes do not fulfill the momentum equilibrium.

At last utilizing the corrected pressure and velocity fields, the energy will be solved. Iterative time –advancement scheme is brought under consideration for the time-advancement scheme. Algebraic equations achieved from eqs. (11) And (12) are solved by the step by step method using the TDMA. (Tri-Diagonal Matrix Algorithm).

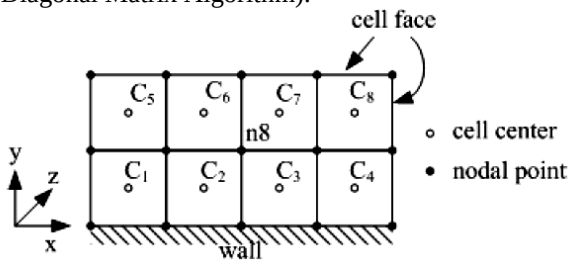

Fig 2 Control volume used to discretize the governing equations.

4.PROBLEM FORMATION AND DESCRIPTION

Two dimensional copper microchannel scheme to be examined in this chapter is demonstrated in fig below that microchannel has 30mm length. Four different channel heights are utilized H_{ch}=1mm, 800µm, 500µm, and 250µm

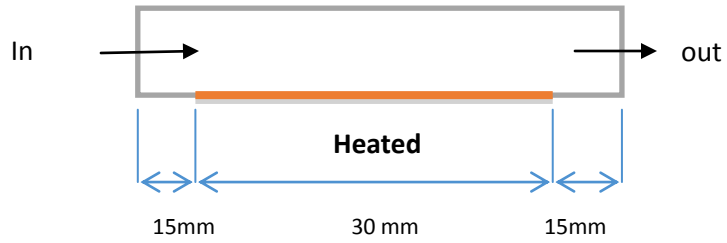

Fig 3: Model of the flow boiling in microchannels

Three constant heat fluxes of 175 kW/m^2, 300 kW/m^2, and 500 kW/m^2 are used another constant heat flux condition is placed only at the outside surface of the bottom channel wall . Initially, subcooled water as the working fluid with a given inlet temperature of Tin = 30 °C and various mass flow rate 1.311 x10^{-6} kg/s and ,3.448x10^{-6} kg/s enter from the inlet plenum to the channel inlet. A mixture of liquid-vapor flow leaves the channel as heat is being added to the working fluid. The thermo physical properties of the working fluid used in the simulation are listed in Table 1

.

Table 1 : Thermophysical properties of working fluid and heat sinks used in computational simulation

Water at T_{in}=30 C^o ,T_{sat}=100 C^o				**Copper**	
ρ_l kg/m^3	958.35	c_{pv} J/kg.K	3768.16	c_{ps} J/kg.K	381
ρ_v kg/m3	0.5982	k_l W/m.K	0.6791	ks W/m.K	387.6
h_{lv} kJ/kg	2256.41	K_v W/m.K	0.0251	ρ_s kg/m^3	8978
c_{pl} J/kg.K	4125.67	μ_l Pa.s	2.8179x10^{-4}		
c_{pv} J/kg.K	3768.16	μ_v Pa.s	1.227x10^{-4}		
k_l W/m.K	0.6791	σ N/m	0.05891		
K_v W/m.K	0.0251	μ_l Pa.s	2.8179x10^{-4}		

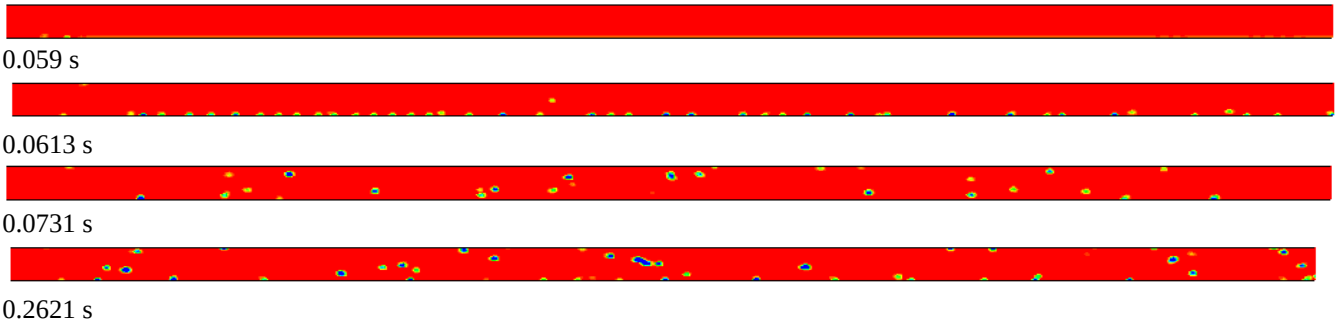

Figure 4. Two-phase flow in 500 µm height microchannel at 3.448x10^{-6} kg/s as a mass flow rate and 500KW/m as a heat flux.

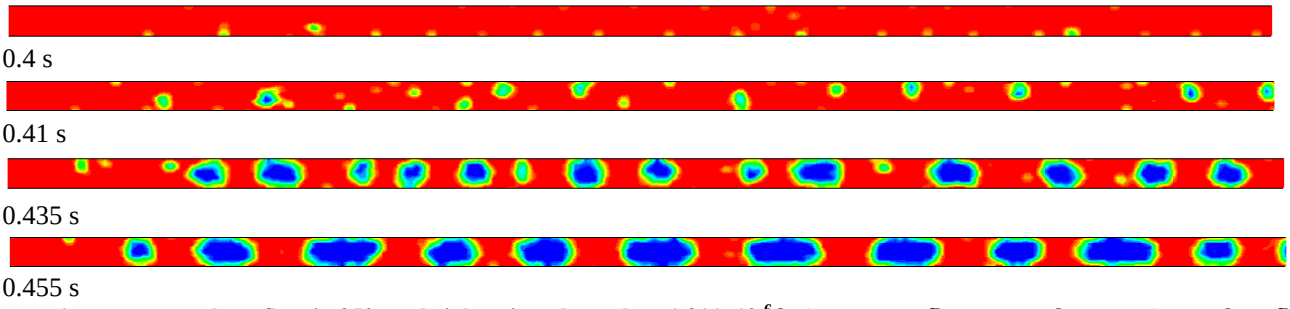

Figure 5. Two-phase flow in 250 µm height microchannel at 1.311x10^{-6} kg/s as a mass flow rate and 175KW/m as a heat flux.

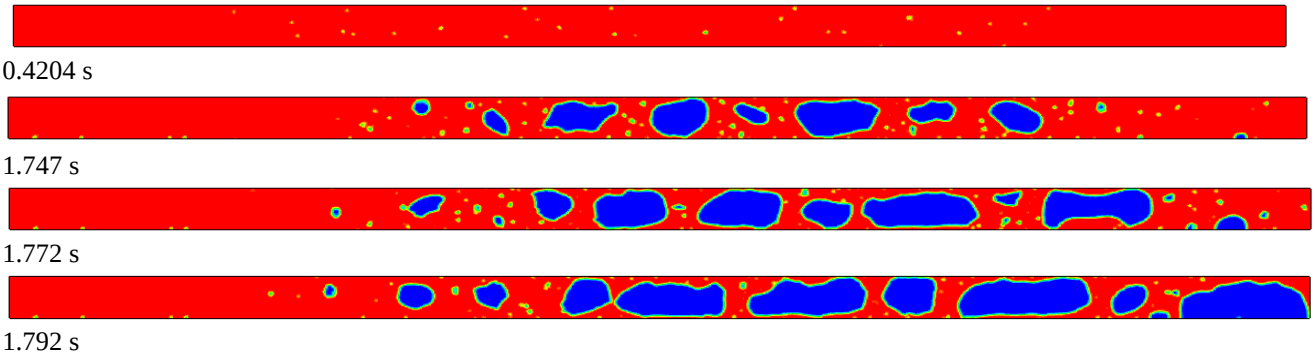

Figure 6. Two-phase flow in 1000 µm height microchannel at 1.311x10^{-6} kg/s as a mass flow rate and 175KW/m as a heat flux

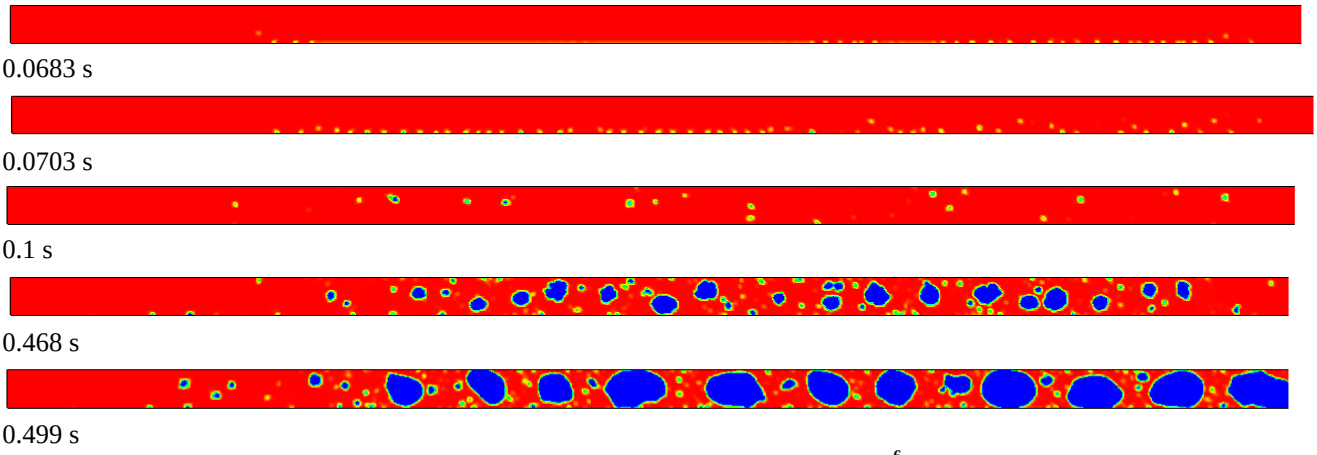

Figure 7. Two-phase flow in 800 µm height microchannel at 1.311x10^{-6} kg/s as a mass flow rate and 500KW/m as a heat flux

Figure 8. Temperature distribution of 800 µm height microchannel at 3.448x10^{-6} kg/s as a mass flow rate and 300KW/m as a heat flux

5. NUMERICAL SIMULATION :

Utilizing the Fluent software package, 2D double precision temporary solver performs the flow boiling simulation in the microchannel along with volume of fluid (VOF) strategy[15]. In the Fluent package, the ICEM CFD software is used to create and mesh the computational model. Simulation uses a separated slow solver to illustrate the temporary changes of the bubbles. For pressure transclusion, the PRESTO (pressure

staggering option) strategy was utilized and for the energy and momentum equations, QUICK (Quadratic Interpolation for Convective Kinetics) was chosen. The PISO (pressure-implicit with splitting of operators) strategy was selected for pressure-velocity coupling. The ratio of the time step to the resistance of the cell time defined by the Courant number is adjusted to be 0.25 for the calculation of volume fraction. The QUICK formulation which is used to lessen the less-favoring impacts artificial diffusion, is third-order accurate. It can be occurred while using low-order upwind strategies. A very large number of cycles and loops are needed for the computations of the energy and momentum equations. I often takes one and a half month to compute the energy and momentum equations results.Following are the boundary conditions of numerical simulations:

- The volume fraction of the vapor phase α_v is set to be 0 where the fluid sub-cooled temperature and fluid velocity are mentioned at the liquid inlet.
- Gauge pressure is internally used FLUENT. Gauge pressure is actually set as 0 at the outlet. The addition of the gauge pressure and operating pressure is called the Absolute pressure. In this model the default operating pressure value is set to be 1 atm and the absolute pressure at the outlet is set to be 1 atm.
- It is not supposed to be a slip condition on the wall.
- Effects of surface tension are accepted and contact angle θ is shown.
- Constant heat flux is applied only on the bottom wall of the heat sink.
- In a microchannel, other than the bottom wall, the other channel walls are set on an adiabatic condition.
- User Defined Functions (UDFs) sets up the source terms comprising transfer of mass between the liquid and vapor phases via liquid-vapor front look .

6.RESULTS AND DISCUSSION:

The heat dissipation capability of the microchannel with 250 μm,300 ,800 and 1000 μm channel heights, different coolant flow rates are compared in this study to investigate the effect of channel dimension and coolant flow rate on the heat flux dissipated by the flow boiling.Bubble nucleation for flow boiling in a 500 μm height channel with the inlet coolant mass flow rate of $3.448x10^{-6}$ kg/s and 500KW/m heat flux is modeled. Figure 4 illustrates the flow boiling phenomenon inthe channel at different time steps. Liquid phase of water is marked in red while the vapor is marked in blue Flow boiling heat flux presents significant variation along the heated wall. Each ripple stands for a bubble in the microchannel. When the bubble is generated, the heat flux is increased significantly due to the latent heat induced by the phase change. In contrast, heat flux dissipated from the heated wall of single phase flow show significant drop after the entrance region as the thermal boundary layer starts to develop. Bubble nucleation and flow boiling in the smaller channel is examined at the similar mass flow rate as previous configuration. Mass flow rate is maintained at $1.311x10^{-6}$ kg/s and 175KW/m as a heat flux. Figure 5 shows the flow boiling phenomenon in the channel. Comparing with 500 μm, 800 μm and 1000 μm microchannel height configuration, it is observed that the bubbles are further confined in the smaller channel and become elongated in shape. The increased coolant flow velocity and elongated bubble might help to increase the heat transfer.

The mass flow rate in the 800 μm height microchannel is then reduced to $1.311x10^{-6}$ kg/s . As a result, the spacing between gas bubble and liquid slug is smaller as shown in Fig.7. Effectiveheat flux dissipation is also observed to reduce .

Fig 8. Shows the temperature distribution along the microchannel of of 800 μm height microchannel at $3.448x10^{-6}$ kg/s as a mass flow rate and 300KW/m as a heat flux,show a temperature increase with time increasing or boiling occurs.

7.REFERENCES :

1. Shkarah, A.J., et al., *A 3D numerical study of heat transfer in a single-phase micro-channel heat sink using graphene, aluminum and silicon as substrates.* International Communications in Heat and Mass Transfer, 2013. **48**: p. 108-115.
2. Shkarah, A.J., M.Y.B. Sulaiman, and M.R.b.H. Ayob, *Analysis of Boiling in Rectangular Micro Channel Heat Sink.* International Journal of Mechanical, Aerospace, Industrial and Mechatronics Engineering, 2014. **8**(4): p. 784-787.
3. Zhang, L., et al., *Phase change phenomena in silicon microchannels.* International Journal of Heat and Mass Transfer, 2005. **48**(8): p. 1572-1582.
4. Zhang, L., et al., *Measurements and modeling of two-phase flow in microchannels with nearly constant heat flux boundary conditions.* Microelectromechanical Systems, Journal of, 2002. **11**(1): p. 12-19.
5. Cheng, P. and H.Y. Wu, *Mesoscale and Microscale Phase-Change Heat Transfer*, in *Advances in Heat Transfer*, J.P.H.A.B.-C. George A. Greene and I.C. Young, Editors. 2006, Elsevier. p. 461-563.
6. Shkarah, A.J., M.Y.B. Sulaiman, and M.R.B. Hj, *Boiling Two Phase Flow in Microchannels: a Review.* Indian Journal of Science and Technology, 2013. **6**(11): p. 5013–5018.
7. Thome, J.R., V. Dupont, and A.M. Jacobi, *Heat transfer model for evaporation in microchannels. Part I: presentation of the model.* International Journal of Heat and Mass Transfer, 2004. **47**(14–16): p. 3375-3385.
8. Huh, C., J. Kim, and M.H. Kim, *Flow pattern transition instability during flow boiling in a single microchannel.* International Journal of Heat and Mass Transfer, 2007. **50**(5-6): p. 1049-1060.
9. Bogojevic, D., et al., *Two-phase flow instabilities in a silicon microchannels heat sink.* International Journal of Heat and Fluid Flow, 2009. **30**(5): p. 854-867.
10. Megahed, A., *Experimental investigation of flow boiling characteristics in a cross-linked microchannel heat sink.* International Journal of Multiphase Flow, 2011. **37**(4): p. 380-393.
11. Hsu, Y.Y., *On the Size Range of Active Nucleation Cavities on a Heating Surface.* Journal of Heat Transfer, 1962. **84**(3): p. 207-213.

12. Kandlikar, S., G., Mizo, V., Cartwright, M., and Ikenze, E., *Bubble Nucleation and Growth Characteristics in Subcooled Flow Boiling of Water.* National Heat Transfer Conference ,HTD-342 , ASME, 1997: p. 11-18.
13. Patankar, S.V., *Numerical Heat Transfer and Fluid Flow.* Hemisphere Publishing Company, Washington, DC, 1980.
14. Shkarah, A.J., M.Y.B. Sulaiman, and M.R.b.H. Ayob, *Two-phase flow in Micro-Channel Heat Sink Review Paper.* The International Review of Mechanical Engineering (IREME), 2013. **7**(1): p. 231-237.
15. Lebanon, N., FLUENT Inc, *FLUENT 13.0 User's Guide.* 2011.